The frustrated antiferromagnetic Heisenberg model in the presence of a uniform field

1996 J. Phys.: Condens. Matter 8 553

(http://iopscience.iop.org/0953-8984/8/5/006)

J. Phys.: Condens. Matter **8** (1996) 553–568. Printed in the UK

The frustrated antiferromagnetic Heisenberg model in the presence of a uniform field

M Schmidt, C Gerhardt, K-H Mütter† and M Karbach

Physics Department, University of Wuppertal, 42097 Wuppertal, Germany

Received 10 May 1995, in final form 15 November 1995

Abstract. On the basis of a numerical computation of the ground states in the sectors with a given total spin S we study the magnetic properties of the one-dimensional frustrated antiferromagnetic Heisenberg model at zero temperature and at the spin-fluid–dimer phase transition. We find that the magnetization curve $M(B)$ has a quartic-root singularity near saturation, $B \longrightarrow 4$. The longitudinal spin–spin, the dimer–dimer and the transverse spin–spin structure factors develop singularities at the field-dependent momenta $p = p_3(M) = \pi(1-2M)$ and $p = p_1(M) = 2\pi M$, respectively. The type of each of these singularities depends on the frustration parameter and the magnetization M.

1. Introduction

During the last few years quantum spin systems with competing interactions have been investigated by several groups [1–8]. These systems are of interest because of frustration effects which lead to a rich phase structure. In the case of the one-dimensional antiferromagnetic spin-1/2 Heisenberg model with next-to-nearest-neighbour coupling:

$$H(\alpha) = 2\sum_{x=1}^{N}[\boldsymbol{s}(x)\cdot\boldsymbol{s}(x+1) + \alpha\boldsymbol{s}(x)\cdot\boldsymbol{s}(x+2)] \tag{1.1}$$

it has been pointed out by Haldane [1] that the ground-state order changes from a gapless 'spin-fluid phase' for $\alpha < \alpha_c$ to a 'dimer phase' with a finite gap for $\alpha > \alpha_c$. The critical coupling has been found to be $\alpha_c \approx 0.25$. In the dimer phase at $\alpha = 1/2$ the ground state of the model is known to be twofold degenerate [9–11]. Both ground states can be represented as products:

$$|l\rangle = \prod_{x=l,l+2,\ldots}[x, x+1] \qquad l = 1, 2 \tag{1.2}$$

of nearest-neighbour spin-0 wave functions $[x, x+1]$—called 'dimers'. Normalized eigenstates of the momentum operator are given by

$$|q_\sigma\rangle = \frac{1}{\sqrt{2+\sigma(-2)^{2-N/2}}}(|1\rangle + \sigma|2\rangle) \tag{1.3}$$

where

$$q_+ = 0 \qquad q_- = \pi. \tag{1.4}$$

† E-mail: muetter@wpts0.physik.uni-wuppertal.de.

0953-8984/96/050553+16$19.50

On leaving the special point $\alpha = 1/2$ the degeneracy of the ground state is lifted. In the region $0 \leqslant \alpha < 1/2$ the momenta of the ground state and the first excited state are $q = 0$, $q = \pi$ for $N = 4, 8, \ldots$ and $q = \pi$, $q = 0$ for $N = 6, 10, \ldots$, respectively. The total spin of the ground state is $S = 0$; the total spin of the first excited state is $S = 1$ in the spin-fluid phase region $0 \leqslant \alpha < \alpha_c$ and $S = 0$ in the dimer phase region $\alpha_c < \alpha \leqslant 1/2$. Therefore, the critical point $\alpha = \alpha_c$ is characterized by the crossing of the lowest singlet and triplet excitations. The difference in long-range order in the two phases shows up in the spin–spin and dimer–dimer correlators. In this paper we will investigate the corresponding static structure factors:

$$S_j(\alpha, p, M = S/N, N) \equiv 4 \sum_x \exp(\mathrm{i}px)\langle S|s_j(0)s_j(x)|S\rangle \qquad j = 1, 3 \tag{1.5}$$

$$D(\alpha, p, M = S/N, N) \equiv 4 \sum_x \exp(\mathrm{i}px)\Big(\langle S|[\boldsymbol{s}(0)\cdot\boldsymbol{s}(1)][\boldsymbol{s}(x)\cdot\boldsymbol{s}(x+1)]|S\rangle - \langle S|\boldsymbol{s}(0)\cdot\boldsymbol{s}(1)|S\rangle^2\Big) \tag{1.6}$$

in the ground states $|S\rangle$ with definite total spin $S_3 = S$. This enables us to study the zero-temperature properties of the model in the presence of a magnetic field B with magnetization $M(B) = S/N$.

For $S = 0$, $M = 0$, equation (1.5) is known to diverge logarithmically for $p \to \pi$, $N \to \infty$ and $\alpha = 0$:

$$S_j(0, p, 0, \infty) \stackrel{p\to\pi}{\longrightarrow} -a \ln\left(1 - \frac{p}{\pi}\right) \qquad j = 1, 3 \tag{1.7}$$

$$S_j(0, \pi, 0, N) \stackrel{N\to\infty}{\longrightarrow} +a \ln N \qquad j = 1, 3. \tag{1.8}$$

The renormalization group approach of [5] and [9] predicts for the leading behaviour of (1.7) and (1.8) $[-\ln(1 - p/\pi)]^{3/2}$ and $(\ln N)^{3/2}$, respectively. From the momentum dependence [10] (for $p \leqslant 13\pi/14$, $N \leqslant 28$) one expects that the amplitude of the leading term is at most 5% of the linear term $-\ln(1 - p/\pi)$. On the other hand, the size dependence of (1.8) has been investigated recently [11] for large systems (up to $N = 70$) by means of the DMRG, and consistency has been found with a fit of the form $a[\ln(cN/2)]^{3/2}$ with $a = 6.67 \times 10^{-2}$, $c = 25.5$. (See also [12–14].)

It was argued in [2] on the basis of numerical results on rings of up to $N = 20$ that the behaviour (1.7) and (1.8) persists over the whole spin-fluid phase region $\alpha < \alpha_c$. In the dimer phase region $\alpha > \alpha_c$, however, the spin–spin structure factor is expected to be finite. From (1.3) one can compute both structure factors (1.5) and (1.6) for $\alpha = 1/2$, $M = 0$:

$$S_j(1/2, p, 0, N) = \frac{2\sin^2(p/2)}{1 + 2^{1-N/2}} + \frac{N}{1 + 2^{N/2-1}}\delta_{p,\pi} \qquad j = 1, 3 \tag{1.9}$$

$$D(1/2, p, 0, N) = \frac{3}{8}\frac{1 - 2^{4-N/2}\cos p}{1 + 2^{1-N/2}} + \frac{9}{16}\frac{N}{1 + 2^{1-N/2}}\delta_{p,\pi} + \frac{9}{32}\frac{N}{1 + 2^{N/2-2} + 2^{-N/2}}\delta_{p,0}. \tag{1.10}$$

The spin–spin structure factor (1.9) is finite for all momentum values p, including π. On the other hand, the dimer–dimer structure factor (1.10) is finite for $p < \pi$ and jumps to infinity for $p = \pi$, $N \to \infty$, which is the signature for long-range dimer order.

The outline of the paper is as follows: in section 2 we present our results for the spin–spin and dimer–dimer structure factors at $M = 0$ and for various values of the frustration parameter α between 0 and 1/2. In section 3 we compare the magnetization curves for the

unfrustrated ($\alpha = 0$) and the frustrated case at $\alpha = 1/4$, where we expect the transition from the spin-fluid to the dimer phase. The same comparison is given in sections 4 and 5 for the longitudinal spin–spin, the dimer–dimer and the transverse spin–spin structure factors in the presence of an external field. Remarkable structures are found which we interpret as signatures of the phase transition.

2. Structure factors in the spin-fluid and dimer phases at $M = 0$

According to [2], the spin–spin structure factor $S_j(\alpha, p = \pi, M = 0, N)$ is expected to increase linearly with $\ln N$ in the spin-fluid phase region $\alpha < \alpha_c$. Figure 1 shows our results for $N = 4, 6, \ldots, 28$. Indeed one observes an almost linear increase in $\ln N$ with a tiny curvature, which is convex for $\alpha < 0.25$ and concave for $\alpha > 0.25$. The behaviour in the spin-fluid phase region $0 \leqslant \alpha < \alpha_c$ can be parametrized by as follows:

$$S_j(\alpha, \pi, 0, N) = a(\alpha) \ln N + b(\alpha) \frac{1}{N^{\phi(\alpha)}} \qquad j = 1, 3; \alpha < \alpha_c. \tag{2.1}$$

The parameters are listed in table 1.

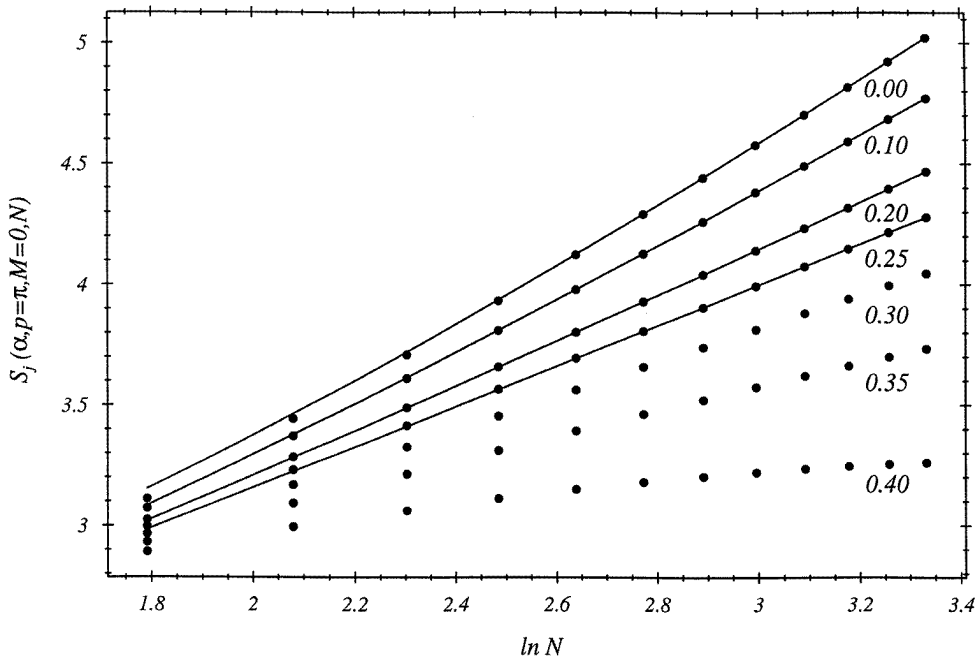

Figure 1. The spin–spin structure factor as a function of the system size N for $\alpha = 0, 0.1, 0.2, 0.25, 0.3, 0.35, 0.4$. The solid curves are fits of the form (2.1).

$a(\alpha)$ and $b(\alpha)$ are quite stable for $\alpha < \alpha_c = 1/4$. At $\alpha = \alpha_c$—where we expect the phase transition—we get $a(1/4) = 0.94(3)$. The exponent $\phi(\alpha)$ approaches zero for $\alpha \to \alpha_c$ and we see a very clean logarithmic behaviour.

We made various attempts to parametrize the size dependence of our numerical results. The *ansatz* (2.1) has the advantage that it reproduces the above-mentioned curvature in a very simple way. No doubt other parametrizations (e.g. including terms of the form $a[\ln(cN/2)]^{3/2}$) are possible as well.

Table 1. Estimated values of the parameters in equation (2.1).

α	$a(\alpha)$	$b(\alpha)$	$\phi(\alpha)$
0.00	1.45	2.21	0.79
0.10	1.33	1.62	0.47
0.20	1.13	1.49	0.23
0.25	0.94	1.50	0.08

In the dimer phase region $\alpha_c < \alpha \leqslant 0.5$ the finite-size behaviour is quite different. From (1.9) we see that finite-size effects drop exponentially at $\alpha = 1/2$. This behaviour seems to persist for $0.4 < \alpha \leqslant 0.5$, but breaks down for smaller values. We were unable to find a few-parameter *ansatz* for the finite-size behaviour in the region $\alpha_c \leqslant \alpha \leqslant 0.4$.

Let us next turn to the dimer–dimer structure factor (1.6). It should be noted that our definition of the dimer–dimer correlators differs from the definition of [2]. The latter is obtained from ours by substituting for the scalar products in (1.6):

$$\boldsymbol{s}(x) \cdot \boldsymbol{s}(x+1) \to s_1(x)s_1(x+1) + s_2(x)s_2(x+1).$$

On the basis of their definition and their results for $N \leqslant 20$ the authors of [2] concluded that the corresponding structure factor increases with N in the dimer phase region $\alpha_c \leqslant \alpha < 1/2$ and with $\ln N$ in the spin-fluid phase region $\alpha < \alpha_c$. Our results for the dimer–dimer structure factor (1.6) at $p = \pi$ on rings with $N = 4, 6, \ldots, 28$ are shown in figures 2(a) and 2(b). In the dimer phase at $\alpha = 0.5$ we observe the behaviour linear in N, as is predicted from (1.10). With decreasing values of α the linear behaviour persists for $0.4 < \alpha \leqslant 0.5$, but the slope becomes flatter. Below $\alpha = 0.4$ a concave curvature emerges for the data points which can be reproduced by the *ansatz*

$$D(\alpha, \pi, 0, N) = c(\alpha) + d(\alpha)N^{\varphi(\alpha)}. \tag{2.2}$$

The parameters are listed in table 2.

Table 2. Estimated values of the parameters in equations (2.2) and (2.3).

α	$c(\alpha)$	$d(\alpha)$	$\varphi(\alpha)$	$\tilde{d}(\alpha)$	$N(\alpha)$
0.00	5.60	−3.32	−0.15	0.86	0.03
0.10	7.39	−5.45	−0.14	1.04	0.12
0.20	21.9	−20.4	−0.05	1.07	0.23
0.25	−16.7	18.0	0.06	0.94	0.25
0.30	−2.23	3.65	0.24	0.53	0.13
0.35	0.80	1.02	0.54	—	—
0.40	2.12	0.30	0.96	—	—
0.45	1.03	0.37	1.05	—	—
0.50	0.17	0.59	0.99	—	—

The exponent $\varphi(\alpha)$ is approximately 1 for $0.4 < \alpha \leqslant 0.5$ and then drops rapidly to zero if we approach the critical point $\alpha \to \alpha_c$. In the spin-fluid phase region $\alpha < \alpha_c$ the exponent $\varphi(\alpha)$ turns out to be negative. This implies that the dimer–dimer structure factor is finite in the spin-fluid phase. At the critical point we expect the exponent $\varphi(\alpha)$ to approach 0. Note also the rapid variations of $c(\alpha)$ and $d(\alpha)$ and the delicate cancellations between the two contributions in (2.2) for $0.2 < \alpha < 0.3$. They are easily understood if we rewrite

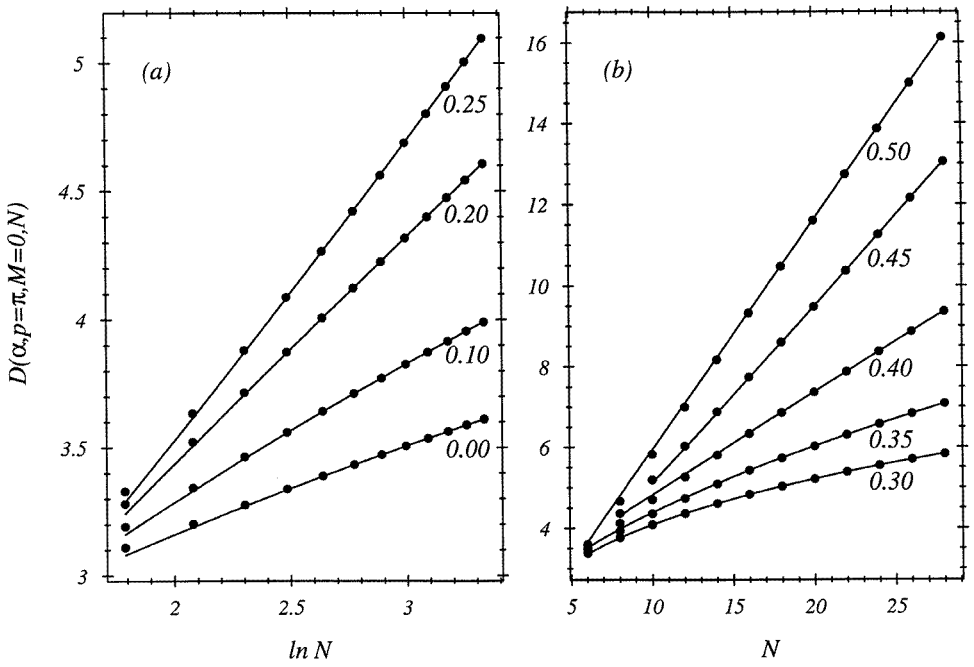

Figure 2. The dimer–dimer structure factor as a function of the system size N. The solid curves are fits of the form (2.2). (a) $\alpha = 0, 0.1, 0.2, 0.25$; (b) $\alpha = 0.3, 0.35, 0.4, 0.45, 0.5$.

(2.2) as follows

$$D(\alpha, \pi, 0, N) = \frac{\tilde{d}(\alpha)}{\varphi(\alpha)}\left(\left(\frac{N}{N(\alpha)}\right)^{\varphi(\alpha)} - 1\right) \tag{2.3}$$

i.e., in terms of the more stable quantities $\tilde{d}(\alpha)$ and $N(\alpha)$, which vary only slowly with α as can be seen in table 2. If (2.3) describes correctly the finite-size behaviour, the critical point with $\varphi(\alpha_c) = 0$ is accompanied with a logarithmic increase of the dimer–dimer structure factor (2.3) with the system size N:

$$D(\alpha_c, \pi, 0, N) \stackrel{N\to\infty}{\longrightarrow} \tilde{d}(\alpha_c) \ln\left(\frac{N}{N(\alpha_c)}\right). \tag{2.4}$$

This is indeed the case as can be seen from figure 2(a). The slope at the critical point $\alpha_c = 1/4$ turns out to be

$$\tilde{d}(1/4) = 1.19(2) \tag{2.5}$$

Let us assume that we have scaling at $\alpha = \alpha_c = 1/4$ in the combined limit

$$N \to \infty \qquad p \to \pi, \qquad z \equiv \left(1 - \frac{p}{\pi}\right) N \text{ fixed.} \tag{2.6}$$

Then we would expect from (2.1) and (2.4) a logarithmic divergence for $p \to \pi$ in both structure factors:

$$S_j(\alpha_c, p, 0, \infty) \stackrel{p\to\pi}{\longrightarrow} -\hat{a}(\alpha_c) \ln\left(1 - \frac{p}{\pi}\right) \qquad j = 1, 3 \tag{2.7}$$

$$D(\alpha_c, p, 0, \infty) \stackrel{p\to\pi}{\longrightarrow} -\hat{d}(\alpha_c) \ln\left(1 - \frac{p}{\pi}\right) \tag{2.8}$$

with the same slopes:

$$\hat{a}(\alpha_c) = 0.91(3) \qquad \hat{d}(\alpha_c) = 1.17(3) \tag{2.9}$$

as found in the finite-size dependence at $p = \pi$. This is indeed the case as can be seen from figure 3, where we have plotted the momentum dependence of all of the structure factors with $N = 8, 10, \ldots, 28$. Away from the critical momentum $p = \pi$, finite-size effects die out rapidly with N^{-2}. Therefore it is rather easy to estimate the thermodynamical limit of the structure factors at noncritical momenta $p < \pi$.

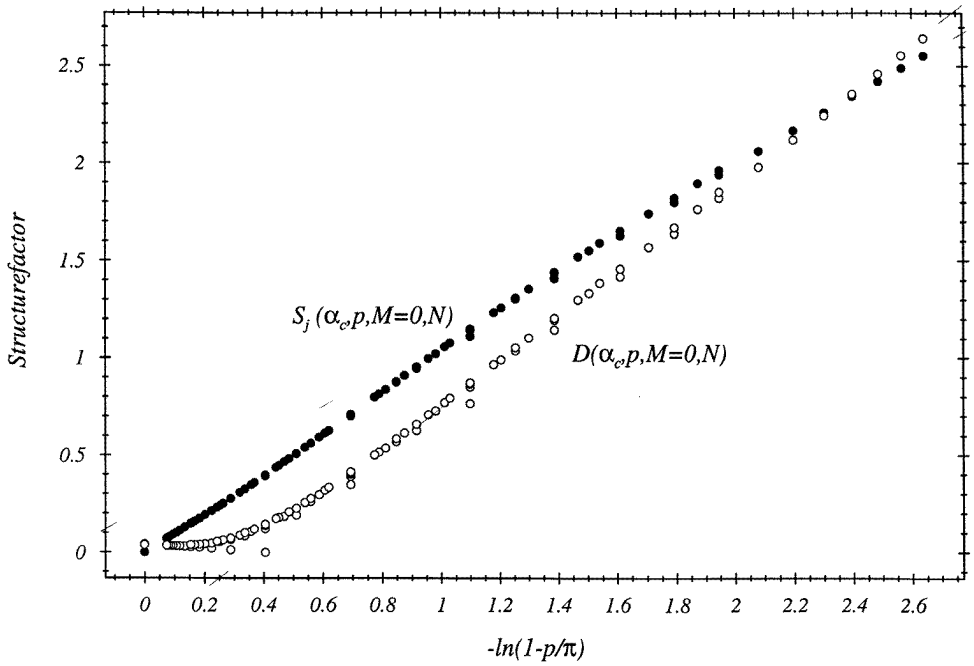

Figure 3. The spin–spin and dimer–dimer structure factors at $\alpha = \alpha_c = 1/4$ versus $-\ln(1 - p/\pi)$.

3. The zero-temperature magnetization curve at $\alpha = \alpha_c$

The difference between the long-range order in the spin-fluid phase and that in the dimer phase has an immediate consequence for the magnetization curve $M = M(\alpha, B) = S/N$ at zero temperature. For $0 \leqslant \alpha \leqslant \alpha_c$ one expects a linear relation between M and B for small external fields B. For $\alpha > \alpha_c$, however, a nonvanishing magnetization demands that the external field exceeds a critical value: $B > B_c(\alpha)$. The magnetization curve of the frustrated AFH model was exploited first by Tonegawa and Harada [15] applying the method of Bonner and Fisher [16] to systems of up to 20 sites. The information on the magnetization curve at $T = 0$ can also be taken from the ground-state energies per site at a given total spin S [17]:

$$\varepsilon(\alpha, M, N) = \varepsilon(\alpha, M) - \frac{\delta(\alpha, M)}{N^{\mu(\alpha, M)}}. \tag{3.1}$$

Once the finite-size effects have been analysed, the magnetization curve follows from

$$\frac{\partial \varepsilon(\alpha, M)}{\partial M} = B(\alpha, M). \tag{3.2}$$

The finite-size behaviour of the ground-state energy per site at $\alpha = 1/4$ and $M = 0$ is of the form N^{-2}, just as it is in the unfrustrated case, $\alpha = 0$. We find for the thermodynamical limit

$$\varepsilon_0 \equiv \varepsilon(1/4, 0) = -0.801\,11(5) \qquad \delta(1/4, 0) = 1.22(2) \qquad \mu(1/4, 0) = 2. \tag{3.3}$$

For small values of M the ground-state energies per site (3.1) scale nicely in an improved scaling variable:

$$(M^*)^2 = M^2 - \frac{1 - 4M^2}{6N^2} \tag{3.4}$$

which was introduced in [17] for the unfrustrated case, $\alpha = 0$. Figure 4 demonstrates that the scaling of the ground-state energies (3.1) works even better in the frustrated case with $\alpha = 1/4$. Therefore we can extract from figure 4 the thermodynamical limit:

$$\varepsilon(1/4, M) = \varepsilon_0(1/4, 0) + \varepsilon_1(1/4, 0)M^2 + \ldots \qquad \varepsilon_1 = 6\delta(1/4, 0). \tag{3.5}$$

From (3.2) and (3.5) we get for the zero-field susceptibility

$$\chi(\alpha_c, 0) \equiv \left.\frac{\partial M(\alpha_c, B)}{\partial B}\right|_{B=0} = \frac{1}{2\varepsilon_1} = \frac{1.35(5)}{2\pi^2} \tag{3.6}$$

which is a a value that is not so different from that of the unfrustrated model ($\chi = 1/2\pi^2$).

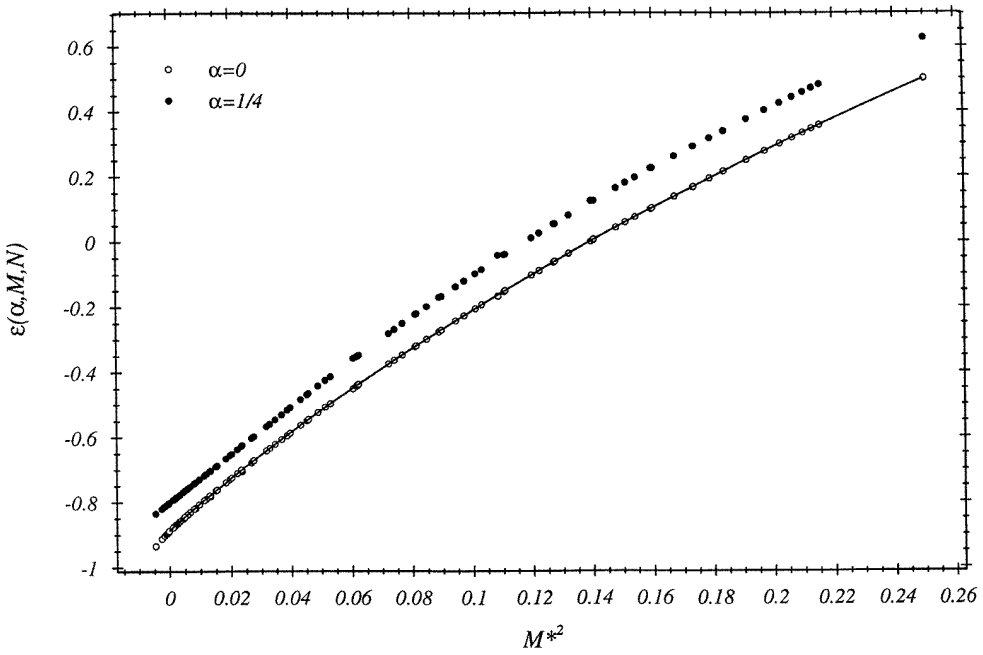

Figure 4. The ground-state energies per site versus the improved scaling variable (3.4) for $\alpha = 0, 1/4$. The solid line is the Bethe *ansatz* solution on a ring with $N = 2048$.

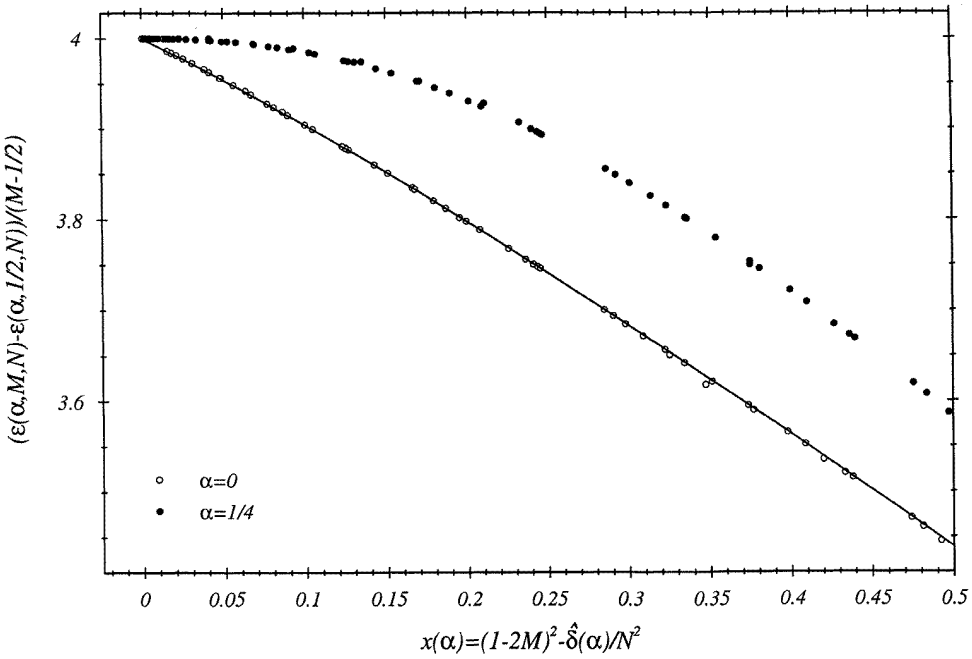

Figure 5. The local derivative (3.7) of the ground-state energies near saturation versus the optimized scaling variable (3.10) for $\alpha = 0, 1/4$. The solid line is the Bethe *ansatz* solution on a ring with $N = 2048$.

Significant differences between the frustrated and unfrustrated model appear in the magnetization curves near saturation $M = 1/2$. These differences are best seen in the local derivative:

$$\frac{\varepsilon(\alpha, M) - \varepsilon(\alpha, 1/2)}{M - 1/2} = 4 - \hat{\varepsilon}_2(\alpha)(1-2M)^2 - \hat{\varepsilon}_3(\alpha)(1-2M)^3 - \hat{\varepsilon}_4(\alpha)(1-2M)^4 + \ldots \tag{3.7}$$

where

$$\varepsilon(\alpha, 1/2) = \frac{1+\alpha}{2} \tag{3.8}$$

is the ground-state energy in the spin sector $S = N/2$. The saturating field B_s is given by

$$\left.\frac{\partial \varepsilon(\alpha, M)}{\partial M}\right|_{M=1/2} \equiv B_s(\alpha, 1/2) = 4. \tag{3.9}$$

Note that the Taylor expansion on the right-hand side of (3.7) starts with the quadratic term in $1-2M$. In the unfrustrated case, $\alpha = 0$, the vanishing of the linear term is known from the result of Yang and Yang [18]. For the frustrated case the validity of the right-hand side of (3.7) can be checked only via numerical results. For this purpose we need an accurate estimate of $\varepsilon(\alpha, M)$ near saturation. In figure 5 we have plotted (3.7) for $N = 6, 8, \ldots, 28$ and $\alpha = 0, 1/4$ versus an 'optimized scaling variable':

$$x(\alpha) = (1-2M)^2 - \frac{\hat{\delta}(\alpha)}{N^2} \tag{3.10}$$

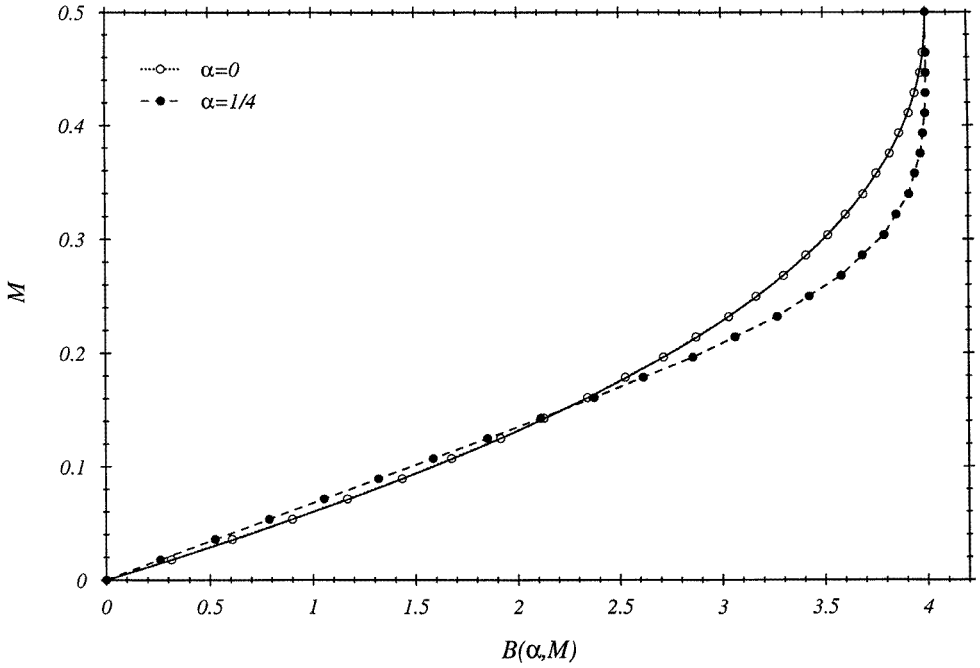

Figure 6. The zero-temperature magnetization curve for $\alpha = 0, 1/4$. The solid line is the Bethe *ansatz* solution on a ring with $N = 2048$.

where

$$\hat{\delta}(0) = 3.5(4) \qquad \hat{\delta}(1/4) = 2.5(4). \tag{3.11}$$

In the unfrustrated case, $\alpha = 0$, one observes a linear behaviour for small values of x with a slope

$$\hat{\varepsilon}_2(0) = 0.90(5) \tag{3.12}$$

which is quite close to the analytic result $\pi^2/12 = 0.82\ldots$ of [18]. For the frustrated case, however, we observe a parabolic behaviour for small values of x:

$$\hat{\varepsilon}_2(1/4) = 0 \qquad \hat{\varepsilon}_3(1/4) = 0 \qquad \hat{\varepsilon}_4(1/4) = 1.70(5). \tag{3.13}$$

Therefore the resulting magnetization curves behave quite differently near saturation, $B \to B_s$:

$$M(0, B) \stackrel{B\to B_s}{\longrightarrow} \frac{1}{2} - \frac{1}{\pi}(B_s - B)^{1/2} \tag{3.14}$$

$$M(1/4, B) \stackrel{B\to B_s}{\longrightarrow} \frac{1}{2} - \frac{1}{2\hat{\varepsilon}_4^{1/4}}(B_s - B)^{1/4}. \tag{3.15}$$

As can be seen in figure 6, this different behaviour is also apparent in the magnetization curves which we computed via the method of Bonner and Fisher [16].

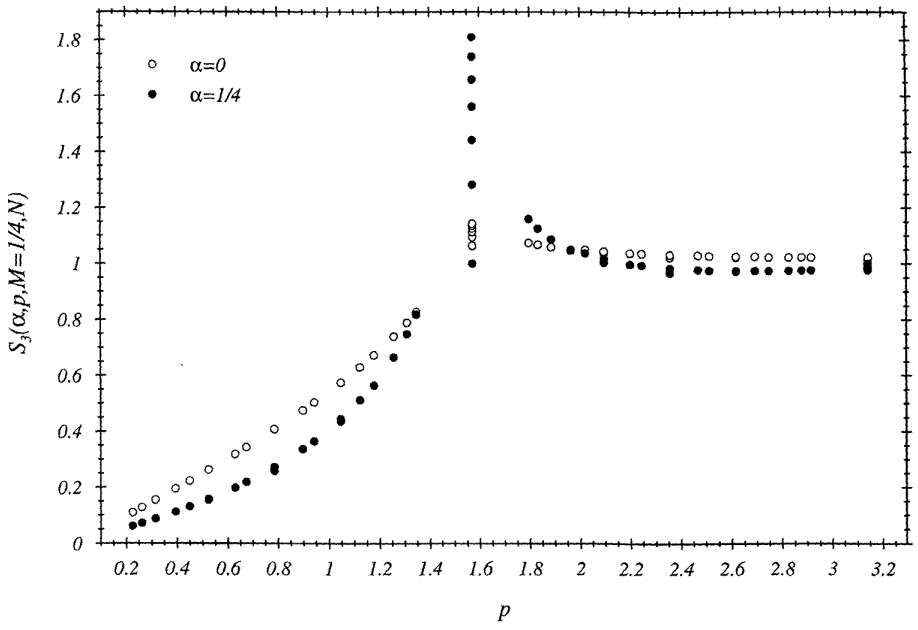

Figure 7. The momentum dependence of the longitudinal spin–spin structure factors at fixed magnetization $M = 1/4$ for $\alpha = 0, 1/4$.

4. Longitudinal spin–spin and dimer–dimer structure factors in the presence of a uniform field at $\alpha = \alpha_c$

The most spectacular difference between the unfrustrated AFH model and the frustrated model at $\alpha = 1/4$ shows up in the longitudinal spin–spin structure factors if we switch on an external field. The unfrustrated case has been treated in [19]. Here we found a cusp singularity—originating from a 'soft mode' [20]—at momenta

$$p = p_3(M) \equiv \pi(1 - 2M) \tag{4.1}$$

where the longitudinal structure factor has its maximum. The maximum value is finite as one can see from a finite-size analysis. The momentum dependence and the finite-size effects of the longitudinal structure factor at $\alpha = 0$ and $M = 1/4$ are shown in figure 7. The situation is completely different in the frustrated case with $\alpha = 1/4$, which is also shown in figure 7. Here the finite-size dependence of the longitudinal structure factor at $p = p_3(M)$ reveals a logarithmic singularity:

$$S_3(1/4,\, p_3(M),\, M,\, N) \overset{N\to\infty}{\longrightarrow} a_c(M) \ln N \tag{4.2}$$

with slopes

$$a_c(M) = \begin{cases} 0.57(5)\text{: } M = 1/6 \\ 0.44(3)\text{: } M = 1/4 \\ 0.23(1)\text{: } M = 1/3 \end{cases} \tag{4.3}$$

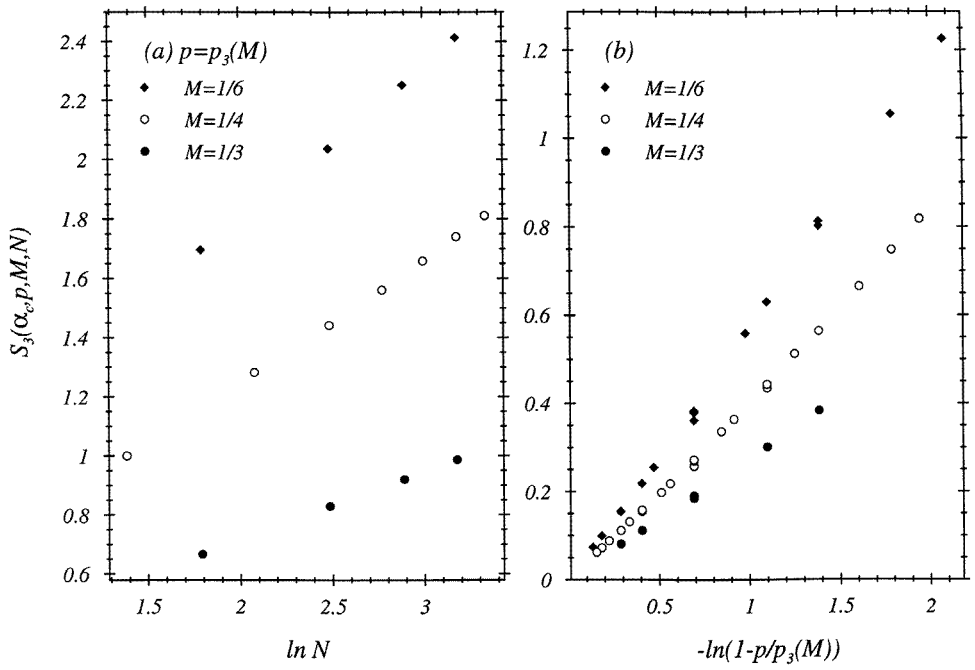

Figure 8. The longitudinal spin–spin structure factor $S_3(\alpha, p, M, N)$ for $\alpha = \alpha_c$ and $M = 1/6, 1/4, 1/3$; (a) at $p = p_3(M)$ versus $\ln N$, (b) versus $-\ln(1 - p/p_3(M))$.

as can be seen from figure 8(a). Approaching the soft mode (4.1) from the low-momentum side $p < p_3(M)$, we observe again a logarithmic singularity in the momentum dependence:

$$S_3(1/4, p, M, \infty) \stackrel{p\to p_3}{\longrightarrow} -\hat{a}_c(M) \ln\left(1 - \frac{p}{p_3(M)}\right) \tag{4.4}$$

as is demonstrated in figure 8(b). The slopes

$$\hat{a}_c(M) = \begin{cases} 0.59(6): M = 1/6 \\ 0.43(4): M = 1/4 \\ 0.27(2): M = 1/3 \end{cases} \tag{4.5}$$

are in remarkable agreement with the slopes (4.3). This indicates that there is scaling in the combined limit

$$p \to p_3(M) \qquad N \to \infty \qquad z_3(M) \equiv \left(1 - \frac{p}{p_3(M)}\right) N \text{ fixed.} \tag{4.6}$$

For large momentum values $p > p_3(M)$ we find an approximate constancy of the longitudinal structure factors in both cases $\alpha = 0$ and $\alpha = 1/4$:

$$S_3(\alpha, p, M, N) = \frac{2}{\pi} p_3(M). \tag{4.7}$$

The interval where (4.7) holds seems to enlarge with increasing values of M and decreasing values of α.

Let us now turn to the dimer–dimer structure factors in the presence of a uniform field. The momentum dependence at fixed magnetization $M = 1/4$ and $\alpha = 0, 1/4$ is shown in

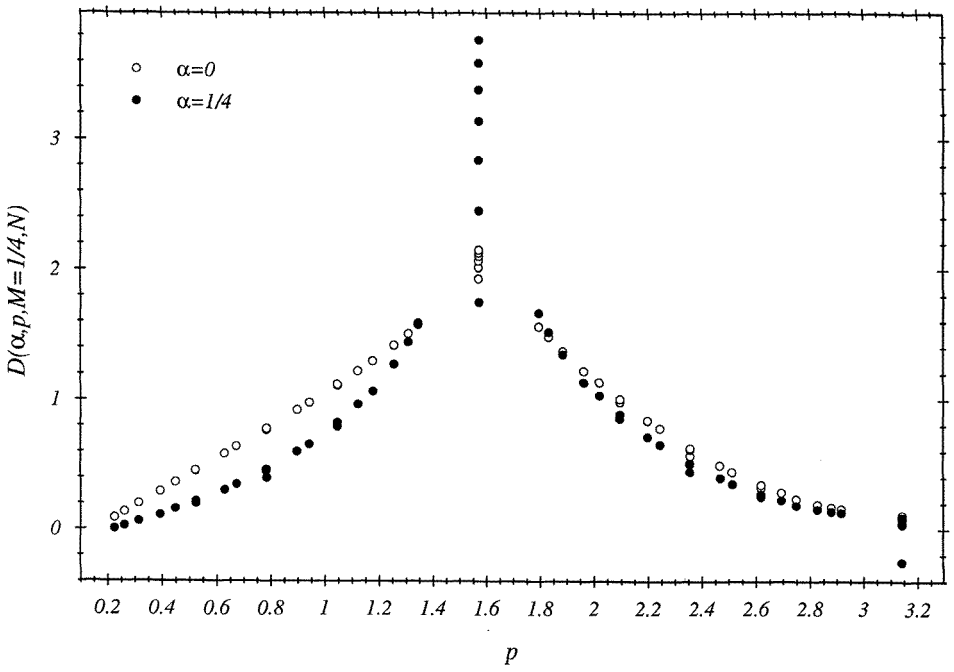

Figure 9. The momentum dependence of the dimer–dimer structure factor at fixed magnetization $M = 1/4$ for $\alpha = 0, 1/4$.

figure 9. We again find a logarithmic increase with the system size N at the soft-mode momentum $p = p_3(M)$ for $\alpha = \alpha_c$:

$$D(1/4,\, p_3(M),\, M,\, N) \stackrel{N\to\infty}{\longrightarrow} d_c(M) \ln N \tag{4.8}$$

with slopes

$$d_c(M) = \begin{cases} 0.70(3)\text{: } M = 1/6 \\ 0.86(5)\text{: } M = 1/4 \\ 0.49(3)\text{: } M = 1/3 \end{cases} \tag{4.9}$$

as can be seen from figure 10(a). From scaling in the combined limit (4.6) we also expect a logarithmic singularity in the momentum dependence:

$$D(1/4,\, p,\, M,\, \infty) \stackrel{p\to p_3}{\longrightarrow} -\hat{d}_c(M) \ln\left(1 - \frac{p}{p_3(M)}\right). \tag{4.10}$$

The slopes

$$\hat{d}_c(M) = \begin{cases} 0.78(3)\text{: } M = 1/6 \\ 0.89(3)\text{: } M = 1/4 \\ 0.82(3)\text{: } M = 1/3 \end{cases} \tag{4.11}$$

can be taken from figure 10(b). The first two agree with the slopes (4.9), which justifies the scaling hypothesis for the dimer–dimer structure factors for the soft mode (4.1) for small values of M. The discrepancy at $M = 1/3$ indicates that the scaling argument does not hold here.

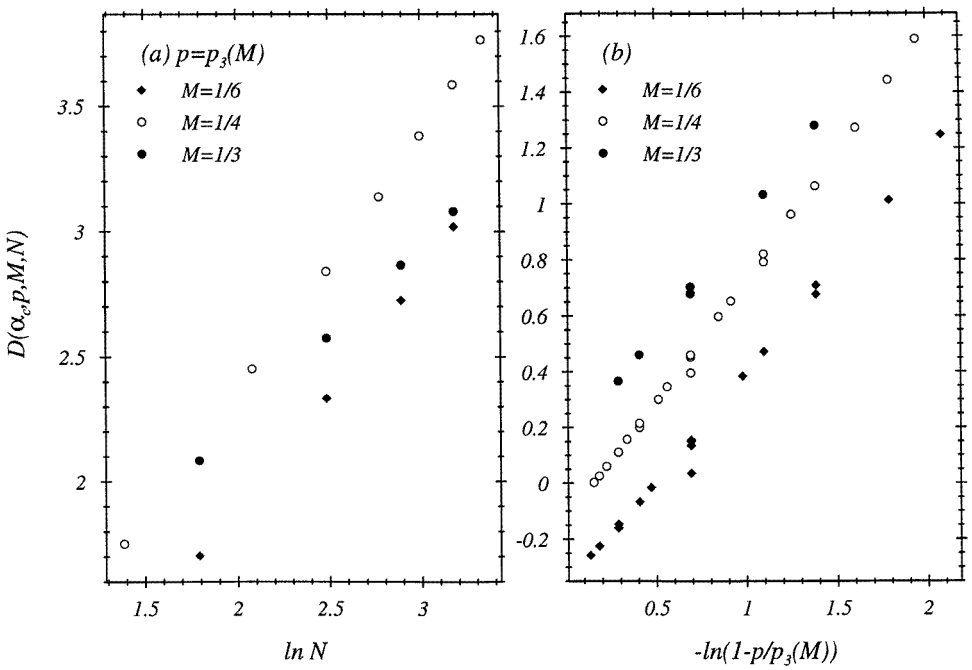

Figure 10. The dimer–dimer structure factor $D(\alpha, p, M, N)$ for $\alpha = \alpha_c$ and $M = 1/6, 1/4, 1/3$; (a) at $p = p_3(M)$ versus $\ln N$, (b) versus $-\ln(1 - p/p_3(M))$.

5. Transverse structure factors in the presence of a uniform field at $\alpha = \alpha_c$

The momentum dependence of the transverse structure factors at fixed magnetization $M = 1/4$ is presented in figure 11 for $\alpha = 0$ and $\alpha = 1/4$, respectively. In contrast to in the longitudinal case, the maximum of the structure factor is found here at $p = \pi$. The almost linear behaviour in $\ln(1 - p/\pi)$ for $\alpha = 0$ signals that the transverse structure factor diverges at $p = \pi$. For $\alpha = 1/4$ the singularity at $p = \pi$ appears to be less pronounced. Note also that the transverse structure factor is almost constant for small momenta:

$$S_1(\alpha, p, M) = \frac{2}{\pi} p_1(M) \qquad p < p_1(M) \equiv 2\pi M. \tag{5.1}$$

At $p = p_1(M)$ we observe a break. Here finite-size effects are larger, as can be seen from the inset in figure 11. They indicate the emergence of a nonanalyticity in the transverse structure factor for the 'soft mode' $p = p_1(M)$. All these features are evident in both cases, $\alpha = 0$ and $\alpha = 1/4$. Differences appear in the finite-size behaviour for the soft mode $p = p_1(M)$. They are larger in the unfrustrated case, $\alpha = 0$, than in the frustrated case, $\alpha = 1/4$. This indicates that the type of the singularity for the soft mode $p = p_1(M)$ changes with the frustration parameter α.

The transverse structure factor at momentum $p = \pi$ versus the magnetization M is shown in figure 12 for the unfrustrated and frustrated cases at $\alpha = 0$ and $\alpha = 1/4$ respectively. The increase with the system size N can be observed for all values of M that are not too large. Therefore we expect from this behaviour as well that the transverse structure factor diverges for $N \to \infty$ and M fixed. The strength of this singularity changes with M and α. In the unfrustrated case, $\alpha = 0$, we see a stronger singularity at $M = 1/4$

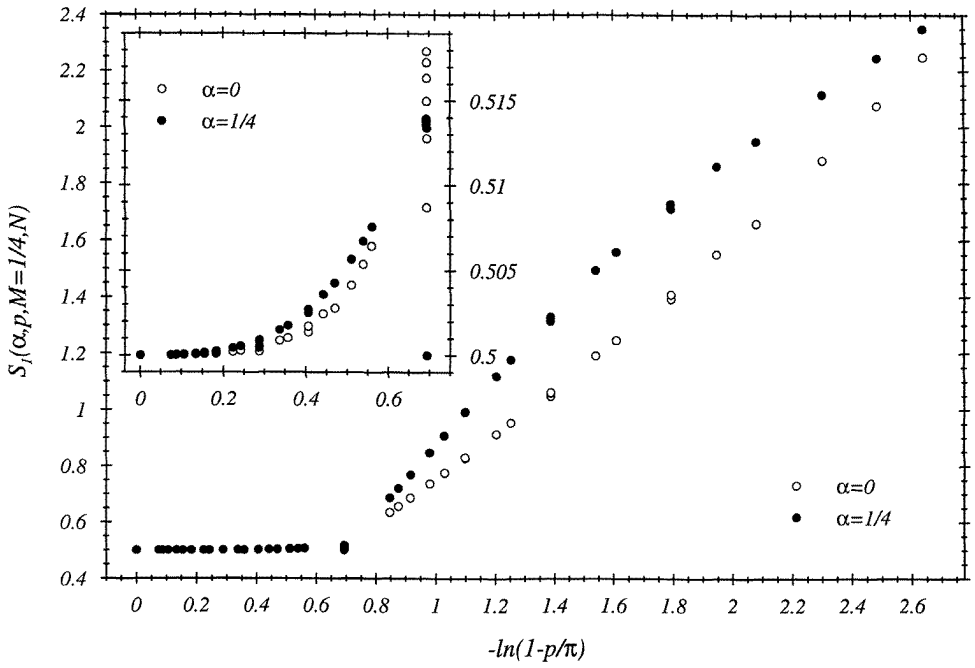

Figure 11. The momentum dependence of the transverse spin–spin structure factor at $M = 1/4$ for $\alpha = 0, 1/4$. The inset is a magnification of the low-momentum behaviour.

than at $M = 0$, which means that a weak magnetic field strengthens the antiferromagnetic order in the transverse structure factor. This strange phenomenon does not occur in the frustrated case at $\alpha = 1/4$.

6. Conclusions

This paper is devoted to an investigation of the spin-fluid–dimer phase transition in the frustrated AFH model (1.1). Signatures for this phase transition have been found before in the level crossing of the first excited states [5] and in the long-range order of the spin–spin and dimer–dimer correlators [2]. We found the most pronounced signatures in the magnetization curve and in the momentum dependence of the spin–spin and dimer–dimer structure factors in the presence of an external field.

(i) The singular behaviour of the magnetization curve near saturation ($B \to 4$) is quite different for $\alpha = 0$ and $\alpha = 1/4$. In the first case one has the well-known square-root behaviour (3.14) first derived in [18]. Our numerical results favour a quartic-root behaviour (3.15) in the magnetization curve of the frustrated model at $\alpha = 1/4$.

(ii) In the presence of an external field with magnetization M the longitudinal spin–spin, the dimer–dimer and transverse spin–spin structure factors develop singularities at field-dependent momenta $p = p_3(M) \equiv \pi(1 - 2M)$ and $p = p_1(M) \equiv 2\pi M$, which are associated with soft modes. For fixed M, the positioning of these singularities is independent of the frustration parameter α. The strength of these soft-mode singularities depends on M and α.

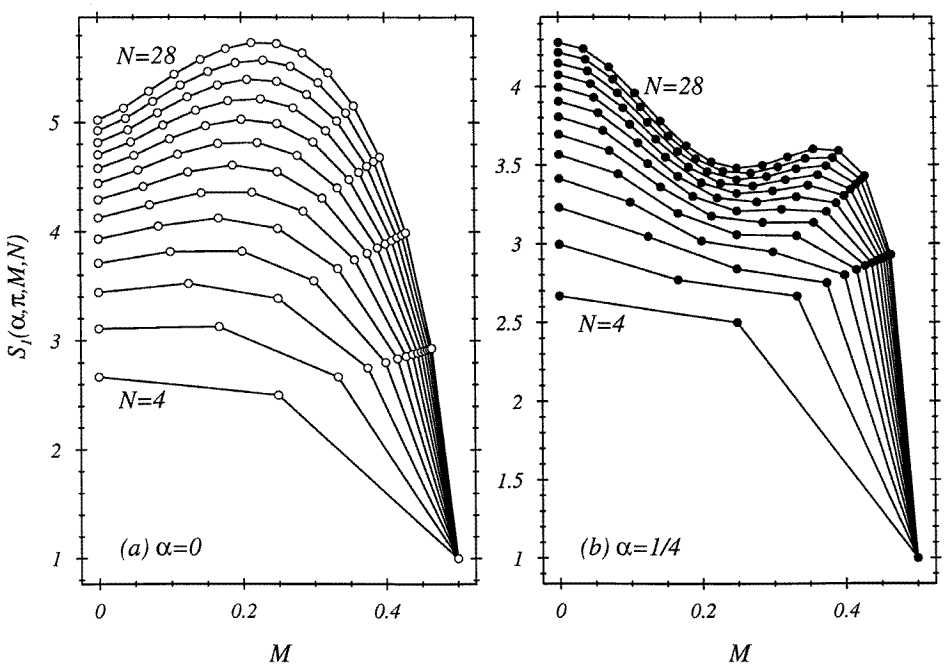

Figure 12. The transverse spin–spin structure factor at $p = \pi$ versus the magnetization M for $N = 4, \ldots, 28$. (a) $\alpha = 0$; (b) $\alpha = 1/4$.

(iii) The longitudinal structure factor has its maximum at the soft-mode singularity $p = p_3(M)$. It is finite and looks like a cusp in the unfrustrated model with $\alpha = 0$. In the frustrated model with $\alpha = 1/4$ we find a logarithmic divergence (4.4).

(iv) The dimer–dimer structure factor at $\alpha = 1/4$ also develops a logarithmic singularity (4.10) for $p \to p_3(M)$.

(v) The soft-mode singularity in the transverse structure factor looks like a break at $p = p_1(M)$. Finite-size effects at this momentum are quite different for $\alpha = 0$ and $\alpha = 1/4$. The transverse structure factor seems to be finite at $p = p_1(M)$, but diverges at $p = \pi$ for fixed M not too large. The strength of this divergence depends on M and α.

Away from the singularities the spin–spin structure factors are rather insensitive to variations of the frustration parameter α. The longitudinal structure factor (4.7) is almost constant for large momenta $p > p_3(M)$ and the transverse one (5.1) is almost constant for low momenta $p < p_1(M)$. Indeed this property seems to be stable against any kind of perturbation. For example, it has also been found in the anisotropic *XXZ*-model [19].

References

[1] Haldane F D M 1982 *Phys. Rev.* B **25** 4925; *Phys. Rev.* B **26** 5257 (erratum)
[2] Tonegawa T and Harada I 1987 *J. Phys. Soc. Japan* **56** 2153; 1988 *Proc. Int. Conf. on Magnetism, J. Physique Coll. Suppl.* **49** C8 1411
[3] Igarashi J and Tonegawa T 1989 *Phys. Rev.* B **40** 756; 1989 *J. Phys. Soc. Japan* **58** 2174
[4] Kuboki K and Fukuyama H 1987 *J. Phys. Soc. Japan* **56** 3126
[5] Affleck I, Gepner D, Schulz H J and Ziman T 1989 *J. Phys. A: Math. Gen.* **22** 511
[6] Tonegawa T, Harada I and Igarashi J 1990 *Prog. Theor. Phys. Suppl.* **101** 513

[7] Tonegawa T, Harada I and Kaburagi M 1992 *J. Phys. Soc. Japan* **61** 4665
[8] Okamoto K and Nomura K 1992 *Phys. Lett.* **169A** 433
[9] Singh R R P and Fisher M E 1989 *Phys. Rev.* B **39** 2562
Nomura K 1993 *Phys. Rev.* B **48** 16814
[10] Karbach M, Mütter K-H and Schmidt M 1994 *Phys. Rev.* B **50** 9281
[11] Hallberg K A, Horsch P and Martinez G 1995 *Preprint* Cond-mat 9505132
[12] Majumdar C K and Ghosh D K 1969 *J. Math. Phys.* **10** 1399
Majumdar C K 1970 *J. Phys. C: Solid State Phys.* **3** 911
[13] van den Broek P M 1980 *Phys. Lett.* **77A** 261
[14] Shastry B S and Sutherland B 1981 *Phys. Rev. Lett.* **47** 964
[15] Tonegawa T and Harada I 1989 *Physica* B **155** 379
[16] Bonner J C and Fisher M 1964 *Phys. Rev.* **135** A640
[17] Fabricius K, Karbach M, Löw U and Mütter K-H 1992 *Phys. Rev.* B **45** 5315
[18] Yang C N and Yang C P 1966 *Phys. Rev.* **150** 321, 326
[19] Karbach M, Mütter K-H and Schmidt M 1995 *J. Phys.: Condens. Matter* **7** 2829
[20] Müller G, Thomas H, Beck H and Bonner J C 1981 *Phys. Rev.* B **24** 1429